NOTICE CONCERNING COPYRIGHT RESTRICTIONS

Using TOUGHREACT to Model Reactive Fluid Flow and Geochemical Transport in Hydrothermal Systems

Tianfu Xu, Eric Sonnenthal, Nicolas Spycher, and Karsten Pruess

Earth Sciences Division, Lawrence Berkeley National Laboratory
University of California, Berkeley, CA 94720.

Keywords

Reactive fluid flow, Geochemical transport, TOUGHREACT, Hydrothermal systems, Mineral alteration

ABSTRACT

The interaction between hydrothermal fluids and the rocks through which they migrate alters the earlier formed primary minerals and leads to the formation of secondary minerals, resulting in changes in the physical and chemical properties of the system. We have developed a comprehensive numerical simulator, TOUGHREACT, which considers non-isothermal multi-component chemical transport in both liquid and gas phases. A variety of subsurface thermo-physical-chemical processes is considered under a wide range of conditions of pressure, temperature, water saturation, and ionic strength. The code can be applied to problems in fundamental analysis of the hydrothermal systems and in the exploration of geothermal reservoirs including chemical evolution, mineral alteration, mineral scaling, changes of porosity and permeability, and mineral recovery from geothermal fluids.

Introduction

The interaction between hydrothermal fluids and the rocks through which they migrate alters the earlier formed primary minerals and leads to the formation of secondary minerals, resulting in changes in the physical and chemical properties of the system. These processes have received increasing attention by investigators of hydrothermal alteration, and engineers concerned with geothermal energy exploration and development. By introducing reactive geochemistry into the framework of the existing code TOUGH2 (Pruess et al., 1999), we have developed a comprehensive non-isothermal multi-component reactive fluid flow and geochemical transport simulator, TOUGHREACT.

TOUGHREACT is applicable to one-, two-, or three-dimensional geologic domains with physical and chemical heterogeneity. The code can be applied to a wide range of subsurface conditions. Temperature can range from 0 to 300°C, limited at present by available geochemical databases such as EQ3/6 (Wolery, 1992). Pressures can be from 1 bar (atmospheric pressure) to several hundred bars (at several thousand meter depth). Water saturation can range from completely dry to fully water saturated. Activity coefficients of charged aqueous species are computed using an extended Debye-Huckle equation and parameters derived by Helgeson et al. (1981) (HKF). The model reproduces fairly well the mean activity coefficients determined by Robinson and Stokes (1965) at 25°C up to at least 6M NaCl (Figure 1), 1M $CaCl_2$, 2M $MgSO_4$, and 1M Na_2SO_4. The fit at higher temperatures will be addressed in the future.

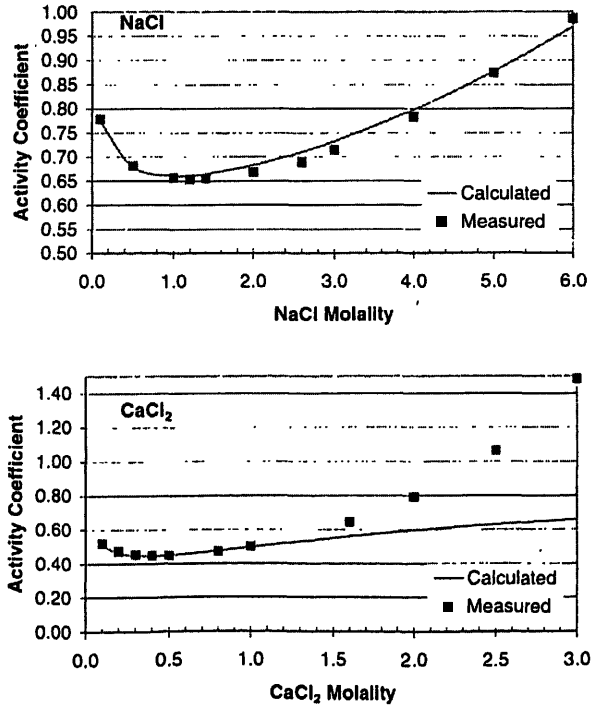

Figure 1. Mean-ion activity coefficients vs. molality for NaCl and $CaCl_2$ solutions. Measured data are from Robinson and Stokes (1965).

In this paper, we give some brief description of features, processes, and applications of the TOUGHREACT code. More details can be found in the user's guide (Xu et al., 2003a). The code is planned to be released to the public in 2003 through the US Department of Energy's Energy Science and Technology Software Center (ESTSC). The TOUGHREACT program modules make use of "self-documenting" features and are distributed with a number of input data files for sample problems. Besides providing benchmarks for proper code installation, these can serve as a self-teaching tutorial in the use of TOUGHREACT, and they provide templates to help jump-start new applications. Like TOUGH2, TOUGHREACT is written in FORTRAN 77. It has been tested on various computer platforms, including PCs, SUN Ultrasparc systems, and Compaq Alpha based workstations. On most machines the code should compile and run without modification.

Major Processes

The treatment of fluid flow and geochemical transport has three important features: (1) the gas phase is active for multiphase fluid flow, mass transport and chemical reactions, (2) reactive fluid flow and transport in fractured rocks as well as porous media can be considered, (3) the effects of heat are considered, including heat-driven fluid flow, and temperature-dependent thermophysical and geochemical properties (such as fluid density and viscosity, and thermodynamic and kinetic data).

Transport of aqueous and gaseous species by advection and molecular diffusion is considered in both liquid and gas phases. Any number of chemical species in liquid, gas and solid phases can be accommodated. Aqueous complexation, acid-base, redox, gas dissolution/exsolution, and cation exchange are considered under the local equilibrium assumption. Mineral dissolution and precipitation can proceed either subject to local equilibrium or kinetic conditions.

Changes in porosity and permeability due to mineral dissolution and precipitation can modify fluid flow. This feedback between flow and chemistry can be important and can be considered in our model, but computational work increases if this is modeled explicitly. Alternatively, the model can monitor changes in porosity and permeability during the simulation from changes in mineral volume fractions without feedback to the fluid flow. Changes in porosity during the simulation are calculated from changes in mineral volume fractions. Several alternative models for the porosity-permeability relationship are included (Xu et al., 2003a).

We currently neglect deformation of the porous skeleton. Heat effects from chemical reactions are neglected in our current model, as are changes in thermophysical properties of fluid phases (such as viscosity, surface tension, and density) due to changes in chemical composition.

Solution Method

TOUGHREACT uses a sequential iteration approach, which solves the flow, transport and reaction equations separately. The flow and transport in geologic media are based on space discretization by means of integral finite differences (IFD; Narasimhan and Witherspoon, 1976). The IFD method gives a flexible discretization for geologic media that allows us to use irregular grids, which is well suited for simulation of flow, transport, and fluid-rock interaction in multi-region heterogeneous and fractured rock systems. An implicit time-weighting scheme is used for individual components of flow, transport, and geochemical reaction. The transport equations are solved independently for each chemical component, whereas the reaction equations are solved on a grid block basis using Newton-Raphson iteration. The quasi-stationary state approximation (Lichtner, 1988) and an automatic time stepping scheme are implemented in TOUGHREACT.

Applications

The TOUGHREACT code was extensively verified against analytical solutions and other numerical simulators (Xu and Pruess, 1998; Xu et al., 1999; Xu and Pruess, 2001b). We have applied the code to a variety of field scale problems. A number of external groups, including Geothermex (Pham et al., 2001), UNOCAL (Ontoy et al., 2003), Japan Electric Power Development Company (Todaka et al., 2003), Ohio State University (Kim et al., 2003), University of Utah, and ExxonMobil, have participated in beta-testing and have used the program for hydrothermal, petroleum reservoir and environmental problems. Here we give some examples of geothermal applications to illustrate applicability of the TOUGHREACT.

Scaling of Hot Brine Injection Wells

Problem Statement

Nag-67 is one of the hot brine injectors located in the south-east of the Tiwi geothermal field, Philippines. The well was completed in March 1987. The well was acidized in January 1989 primarily to clear the near-wellbore formation of drilling mud damage and to improve its injectivity. Injection capacity of the well after the stimulation was 126 kg/s at a wellhead pressure of 1.38 MPa. In 1999, an injectivity test indicated the capacity of the well had reduced to 17 kg/s at an injection wellhead pressure of 1.31 MPa. In March 2000, recorded injection in Nag-67 suddenly dropped to 3.8 kg/s. In January 2001, scale inside the Nag-67 wellbore was drilled-out and the scale deposited in the near-well formation was dissolved by acid. Measurements after the scale drillout indicated that the capacity of the injector went up to 25.2 kg/s, and another test after the acid stimulation showed a further increase to 113.4 kg/s. These results strongly suggested that the decline in injectivity of the well was caused primarily by scale deposition in the near-well formation. Numerical analyses were carried out to investigate scaling mechanisms in the formation.

Mesh Setup and Fluid Flow Parameters

The formation region at the bottommost permeable zone of Nag-67 was modeled. This zone extends over a thickness of 120 m. A simple one-dimensional radial flow model was used, consisting of 50 radial blocks with logarithmically increasing radii (Figure 2).

Only the fracture network (assumed to represent 1% of the total formation volume) is considered in the model, with the assumption that the fluid exchange with the surrounding low permeability matrix is insignificant. Heat transfer between fracture

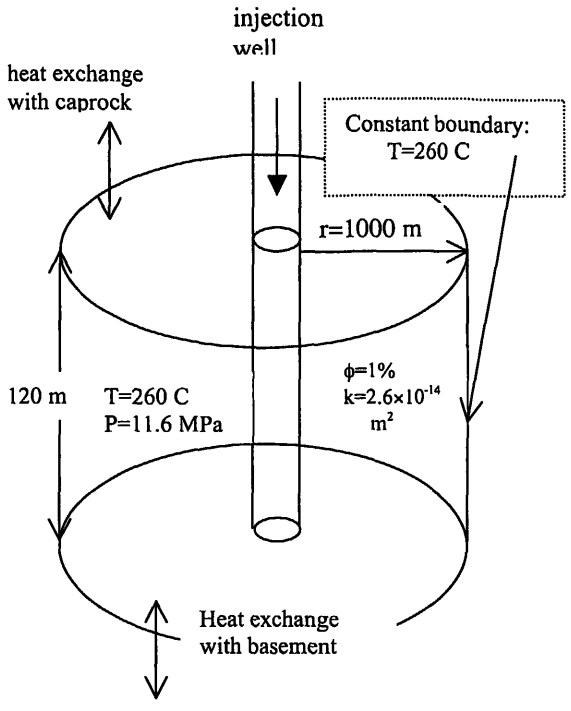

Figure 2. Simplified conceptual model for injection well Nag-67.

and matrix was accounted for by allowing heat exchange with assigned confining layers. The injection history of the well was used to define the amount of injected mass versus time: 50% of the total injection rate in Nag-67 was assigned to the bottommost permeable zone because spinner surveys showed that the zone accepted 50% of the injectate.

Geochemical Data

Based on the chemistry of the brine injected and analysis of some scale deposited, the majority of scale in Nag-67 was determined to be amorphous silica. From the historical chemical record, the degree of amorphous silica saturation in each analyzed water sample was determined (as ppm SiO_2 above the amorphous silica solubility at the temperature of the sampled brine). Using the data of Gunnarsson and Arnorsson (2000) for amorphous silica solubility, the average degree of supersaturation in the injected brine over time was estimated to be around 10 ppm (as SiO_2), and ranging between −100 ppm (i.e., undersaturated) and +200 ppm. A supersaturation of 10 ppm SiO_2 was calculated to correspond to a typical brine temperature of 160°C.

The initial abundances of primary minerals were determined from the reported Nag-67 alteration mineralogy at the 1798-1920 m MD permeable zone (propylitic/phyllic rock, Table 1). Secondary minerals were also determined from field observations. The composition of the injected brine was provided from historical analytical data. Calcite and anhydrite were assumed to be at local equilibrium because their reaction rate is typically quite rapid. Other minerals were set to react under kinetic constraints. Thermodynamic and kinetic data for amorphous silica were taken from Gunnarsson and Arnorsson (2000) and Carroll et al., (1998), as mentioned earlier. For other minerals, thermodynamic and kinetic data were taken from various other literature sources.

Table 1. Minerals and aqueous species considered in the model for injection well Nag-67.

Mineral	Mineral Precipitation/ Dissolution	Mineral Initial Volume fraction	Primary Aqueous Components
Primary:			
albite-low	Kinetic	0.18	H_2O
anorthite	Kinetic	0.02	H^+
illite	Kinetic	0.05	Ca^{+2}
quartz	Kinetic	0.14	Mg^{+2}
muscovite	Kinetic	0.16	Na^+
clinochlore-7A	Kinetic	0.08	Cl^-
clinozoisite	Kinetic	0.01	$SiO_2(aq)$
calcite	Equilibrium	0.13	HCO_3^-
			SO_4^{-2}
Secondary:			K^+
amorphous silica	Kinetic		AlO_2^-
microcline	Kinetic		
kaolinite	Kinetic		
anhydrite	Equilibrium		

Factors that were identified to possibly have an effect on scale formation are (1) the silica concentration in the hot brine injectate, (2) the temperature of the injectate, (3) the flowrate of the injectate, (4) the pH of the injectate, and (5) the temperature and pressure conditions of the reservoir in the vicinity of the injector. A number of simulations were performed to test how these factors influence scale formation. Simulations were carried out for ten years of continuous injection. Only two simulations results are presented here, each using a different injection temperature (152, 160°C), but the same SiO_2 concentration in the injected brine (752 ppm) and same initial reservoir temperature (260°C).

Results

Significant amount of amorphous silica precipitates at the lower injectate temperature of 152°C (Figure 3a). At this temperature, the silica concentration in the brine exceeds the solubility of amorphous silica by approximately 100 ppm. At 160°C, the solubility of amorphous silica is exceeded by 50 ppm and, accordingly, less silica is precipitated. The precipitation occurs within the first 50 meters from the injector. Accordingly, porosity and permeability are changed (Figure 3b). At 152°C, the precipitation of amorphous silica and other minerals results in a decrease in fracture void volume by up to 12%. The corresponding permeability decrease close to the borehole is calculated to be about one order of magnitude. We used a porosity-permeability relationship presented by Verma and Pruess (1988).

$$\frac{k}{k_0} = \left(\frac{\phi - \phi_c}{\phi_0 - \phi_c}\right)^n \quad (1)$$

where ϕ_c is the value of "critical" porosity at which permeability goes to zero, and n is a power law exponent. Parameters ϕ_c and n are medium-dependent. Here, we arbitrarily chose $\phi_c = 0.42$ and $n = 1.5$. Using such a relationship, the trend between observed and simulated injection rates and pressures is captured. However, further studies would be required to calibrate parameters ϕ_c and n to field data.

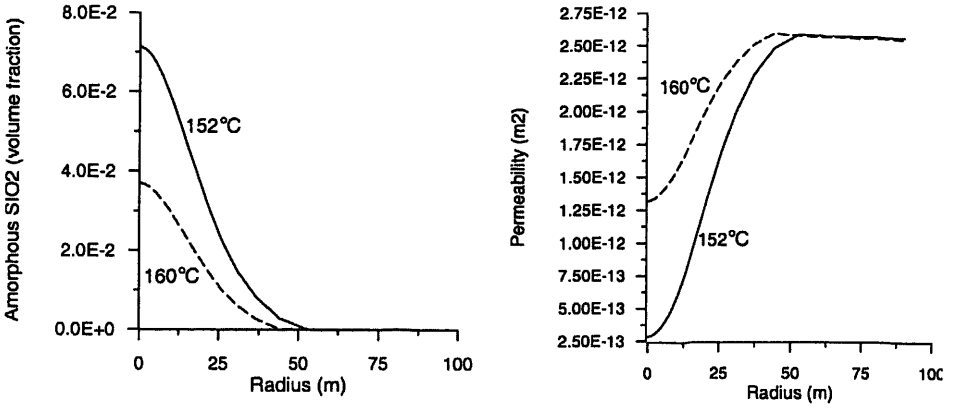

(a) Precipitation of amorphous silica

(b) Permeability distribution

Figure 3. The precipitation of amorphous silica and permeability distribution after 10 years.

The results of numerical simulation reported here are preliminary. More accurate predictions of injectivity loss would be obtained using refined permeability-porosity relationships. Also, the modeling effort could benefit from a more rigorous formulation of silica precipitation kinetics. Nevertheless, integrating simple numerical simulations as described here provided a useful insight into operational constraints and factors controlling silica deposition around a typical geothermal injection well. Additional information is available in Ontoy et al. (2003).

Geothermal Alteration due to Mixing of Acidic and Neutral Fluids

Problem Statement

Two types of fluids are encountered in the Onikobe geothermal reservoir, one neutral and the other acidic. The acidic fluid is characterized by higher concentrations of Mg, Fe, Pb, Zn, and Cl compared with the neutral one (Table 2). The two types of fluids are locally isolated from one another. Based on a spatial relationship between the acidic fluid zone and acidic alteration (pyrophyllite) zone, it is determined that acidic fluid might be upwelling along the fault. Mn-rich smectite scale coexisting with sulfides (pyrite, sphalerite and galena) armed the inside of some production wells by mixing of acidic and neutral fluids (Todaka and Tezuka, 2002). In order to test the hypothesis that acidic fluid might be upwelling along a fault zone and that an impermeable barrier might be present between the acidic and neutral fluid zones, a 1-D conceptual model was used.

Hydrogeological Conditions

The 1-D porous medium model is shown in Figure 4. Rock properties used are as follows: grain density: 2750 kg/m^3, porosity: 0.2, permeability: 1×10^{-16} m^2, thermal conductivity: 3 W/(m°C), heat capacity: 1000 J/(kg°C). The temperature and pressure conditions were from field data. A total of 100 grid blocks was used.

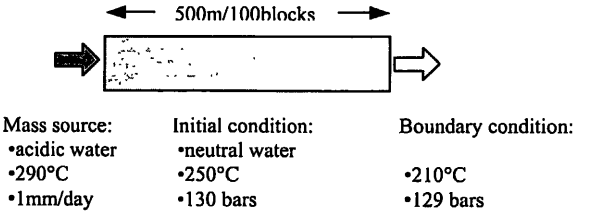

Figure 4. Schematic represemntion of the flow model.

Darcy velocity was set to 1 mm/day by specification of the mass source in the left boundary block. A linear temperature gradient from 290°C to 210°C is assumed in the non-isothermal flow model, to evaluate temperature effects in reactive geochemical transport.

Table 2. List of initial and boundary water chemical compositions, initial mineral volume fractions and possible secondary mineral phases used in the simulations.

Water composition (mol/kg)			Initial mineral abundance			
Component	Initial neutral water (well 134)	Boundary acidic water (well 130)	Primary	Volume fraction	Secondary	Volume fraction
pH	5.5	3.4	quartz	0.1477	clinochlore	0.0
Cl^-	4.442×10^{-2}	9.909×10^{-2}	K-feldspar	0.0495	daphnite	0.0
SO_4^{2-}	6.500×10^{-3}	1.150×10^{-2}	albite	0.2232	illite	0.0
HCO_3^-	1.372×10^{-2}	1.782×10^{-2}	anorthite	0.3145	kaolinite	0.0
$SiO_2(aq)$	8.498×10^{-3}	8.428×10^{-3}	diopside	0.0149	pyrophyllite	0.0
Al^{3+}	5.656×10^{-6}	9.577×10^{-6}	hedenbergite	0.0098	laumontite	0.0
Ca^{2+}	3.098×10^{-3}	1.127×10^{-2}	enstatite	0.0736	wairakite	0.0
Mg^{2+}	5.992×10^{-6}	1.143×10^{-3}	ferrosilite	0.0493	prehnite	0.0
Fe^{2+}	1.491×10^{-6}	2.214×10^{-3}	magnetite	0.0176	clinozoisite	0.0
K^+	3.814×10^{-3}	7.412×10^{-3}			epidote	0.0
Na^+	3.470×10^{-2}	6.228×10^{-2}	porosity	0.1	Mn-smectite	0.0
Mn^{2+}	2.399×10^{-6}	5.784×10^{-5}	total	1.0	pyrite	0.0
Zn^{2+}	1.061×10^{-7}	3.376×10^{-5}			sphalerite	0.0
Pb^{2+}	1.000×10^{-12}	5.899×10^{-6}			galena	0.0
					calcite	0.0
Temp (°C)	250	254			anhydrite	0.0

Geochemical Conditions

The neutral fluid has a pH of 5.5 under reservoir conditions; it is called neutral in this paper because the water at the separator is neutral under ambient conditions. Water from well 134 is selected as representative of initial water (neutral) and the acidic fluid (pH = 3.4) from well 130 as boundary water. Chemical concentrations of the two waters (Table 2) are calculated from separated waters (equal to re-injected water) and vapors from well 134 and well 130 using their total enthalpies. Initial mineral abundances considered are also listed in Table 2. Possible secondary minerals were determined from field and experimental observations of water-rock interaction and from equilibrium geochemical model calculations. Calcite and anhydrite dis-

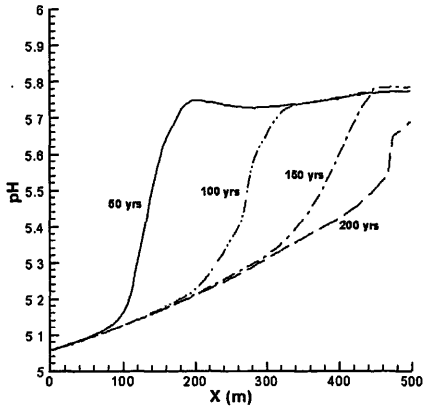

Figure 5. Water pH distribution in the 1-D model.

solution and precipitation were assumed to occur under chemical equilibrium, whereas those of the other minerals were considered under kinetic conditions.

Results

Water pH distribution is presented in Figure 5. Mn-rich smectite precipitates near the mixing front (Figure 6a), and then dissolves by acidic water displaced with time due to the pH decrease. The movement of the Mn-rich smectite peak is consistent with the pattern of pH. Precipitation of pyrite (Figure 6b) and sphalerite occurs near the mixing front, and their precipitation peaks move with the mixing front. The precipitation peaks of Mn-rich smectite and sulfide minerals increase as temperatures decrease. Scale of Mn-rich smectite and sulfide minerals in the Onikobe production well was observed by Ajima et al. (1998). Mn-rich smectite precipitation is also observed at a depth where neutral fluid mixes with acidic fluid rising from deep feed zone in the Onikobe production wells (Ajima et al., 1998). The observed mineral assemblages have been reproduced by the simulation. Precipitation of Mn-rich smectite tends to decrease porosity and permeability, and it is likely to form an impermeable barrier between regions with acidic and neutral fluids over geologic time periods. Further discussion is given in Todaka et al. (2003).

Other Applications

Other major TOUGHREACT application examples are summarized in Table 3, overleaf. These examples include (1) mineral recovery from geothermal fluids (Problem 1 in Table 3, overleaf), and (2) thermal-hydrodynamic-chemical processes in natural hydrothermal systems (Problems 2 and 3), (3) mineral deposition such as supergene copper enrichment (Problem 4), (4) assessment of nuclear waste disposal sites (Problems 5 and 6), (5) sedimentary diagenesis and CO_2 disposal in deep geologic formations (Problem 7), and (6) natural groundwater quality evolution and contaminant transport under ambient conditions (Problem 8).

Conclusions

A non-isothermal reactive fluid flow and geochemical transport code, TOUGHREACT, has been developed by introducing reactive geochemistry into the framework of the existing widely used geothermal reservoir simulator TOUGH2. TOUGHREACT includes comprehensive chemical interactions between liquid, gaseous and solid phases that are coupled to solute transport and subsurface multiphase fluid and heat flow. The code can be applied to a wide range of problems in geothermal reservoir engineering and for fundamental analyses of hydrothermal systems, which include: (1) chemical evolution and mineral alteration under natural and production conditions, (2) mineral scaling and changes of porosity and permeability due to injection and/or production, (3) mineral recovery from geothermal fluids. The applicability of the code to geothermal problems has been illustrated by several examples. TOUGHREACT can be also applied to other problems such as mineral deposition, assessment of nuclear waste disposal sites, sedimentary diagenesis, CO_2 disposal in deep geologic formations, natural groundwater quality evolution, and contaminant transport under ambient conditions.

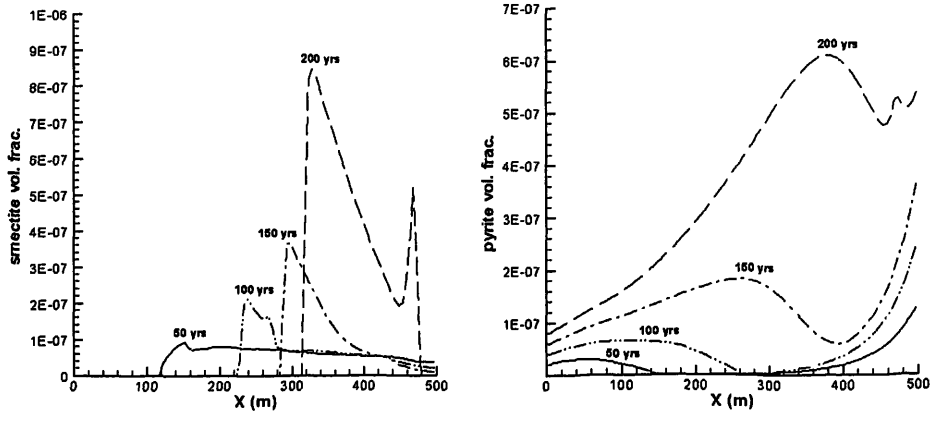

(a) Mn-semctite (b) Pyrite

Figure 6. Changes of mineral volume fraction in the model.

Acknowledgment

We acknowledge Carol Bruton for her suggestions and comments during the review process. This work was supported by the Assistant Secretary for Energy Efficiency and Renewable Energy, Office of Wind and Geothermal Technologies, of the U.S. Department of Energy, under Contract No. DE-AC03-76SF00098.

References

Ajima, S., N. Todaka, and H. Murakake, 1998. An interpretation of smectite precipitation in production wells caused by the mixing of different geothermal fluids. *In proceedings of 23rd Workshop on Geothermal Reservoir Engineering, Stanford University*, 264-269.

Table 3. List of major TOUGHREACT application examples.

Problem	*Description*	*Model system*	*Reaction type*	*Reference*
1. Recovery of minerals from geothermal brines	Commercial recovery of minerals from geothermal brines is being practiced at the Salton Sea field in the Imperial Valley of California. The processes are affected by chemical processes within the reservoir.	2-D, 50 grid blocks, 2 minerals, 23 aqueous species	Aqueous complexation, Redox, Mineral dissolution/ exsolution	Pham et al., 2001
2. Thermal-hydrodynamic-chemical processes in natural hydrothermal systems.	Chemical compositions of geothermal fluids from 14 geothermal fields in Japan and Kamchatka (Russia) were used to model thermo-hydrodynamic-chemical processes.	1-D flow tube model, 21 minerals, 31 aqueous species, 1 gas (CO_2)	Aqueous complexation, Mineral dissolution/ precipitation, Gas dissolution/exsolution	Kiryukhin et al., 2002
3. Caprock hydrothermal alteration	The observed sequence of argillic alteration in the Long Valley Caldera, California, consists of an upper zone with smectite and kaolinite, a lower illite zone, and an intermediate mixed illite and smectite zone. The sequence is reasonably well reproduced in the numerical simulation.	2-D with fracture-matrix interaction. 742 grid blocks, 14 minerals, 23 aqueous species, 1 gas (CO_2)	Aqueous complexation, Mineral dissolution/ precipitation, Gas dissolution/exsolution	Xu and Pruess (2001a)
4. Supergene copper enrichment (SCE)	Oxidative weathering of pyrite (FeS_2) and chalcopyrite ($CuFeS_2$) causes acidification and mobilization of metals in the unsaturated zone and intense alteration of primary minerals, with subsequent formation of enriched secondary copper-bearing sulfide mineral deposits (enrichment blanket) in the reducing conditions below the water table.	2-D, 77 grid blocks, 18 minerals, 46 aqueous species, 1 gas (O_2)	Aqueous complexation, Redox, Mineral dissolution/ precipitation, Gas dissolution/exsolution	Xu et al. (2001)
5. Effects of thermohydrology on geochemistry	The problem is investigated for the Drift Scale Test (DST), in which a strong heat source is emplaced in unsaturated fractured volcanic tuffs at Yucca Mountain, Nevada.	2-D with fracture-matrix interaction, 3000 grid blocks 22 minerals, 28 aqueous species, 1 gas (CO_2)	Aqueous complexation, Mineral dissolution/ precipitation, Gas dissolution/exsolution	Spycher et al. (2003)
6. Calcite precipitation and infiltration fluxes at Yucca Mountain	Using reaction-transport model to investigate the relationship between percolation flux and measured calcite abundances.	1-D column with fracture-matrix, 130 grid blocks, 22 minerals, 28 aqueous species, 1 gas (CO_2)	Aqueous complexation, Mineral dissolution/ precipitation, Gas dissolution/exsolution	Xu et al. (2003c)
7. Mineral trapping for CO_2 disposal in deep saline aquifers	Simulations were performed for a commonly encountered Gulf Coast sediment under natural and CO_2 injection conditions in order to analyze the impact of CO_2 immobilization through carbonate mineral precipitation.	1-D radial, 130 grid blocks, 22 minerals, 28 aqueous species, 1 gas (Supercritical CO_2)	Aqueous complexation, Mineral dissolution/ precipitation, Gas dissolution/exsolution	Xu et al. (2003b)
8. Water quality in the Aquia aquifer, Maryland	$NaHCO_3$ type waters in the coastal plain aquifers of the eastern United States have been related to freshening of the aquifer. The water quality in this aquifer shows zonal bands with changes in concentrations of major cations that have been attributed to cation exchange and calcite dissolution/precipitation.	1-D, 16 grid blocks, 1 mineral, 20 aqueous species, 5 exchanged cations	Aqueous complexation, Mineral dissolution/ precipitation, Cation change	Xu and Pruess (1998)

Carroll, S., E. Mroczek, M. Alai, and M. Ebert, 1998. Amorphous Silica Precipitation (60 to 120°C): Comparison of Laboratory and Field Rates. *Geochimica et Cosmochimica Acta*, v.62(8), p.1379-1396.

Gunnarsson, I., and S. Arnórsson, 2000. Amorphous silica solubility and the thermodynamic properties of H_4SiO_4 in the range of 0° to 350°C at P_{sat}. *Geochimica et Cosmochimica Acta*, v.64 (13), p.2295-2307.

Helgeson, H. C., D. H. Kirkham, G. C. Flowers, 1981. Theoretical prediction of the thermodynamic behavior of aqueous electrolytes at high pressures and temperatures: IV. Calculation of activity coefficients, osmotic coefficients, and apparent molal and standard and relative partial molal properties to 600 C and 5 kb. *American Journal of Science*, v. 281, p. 1249–1516.

Lichtner, P. C., 1988. The quasi-stationary state approximation to coupled mass transport and fluid-rock interaction in a porous medium, *Geochimica et Cosmochimica Acta*, v.52, p.143-165.

Kiryukhin, A., T. Xu , K. Pruess , and I. Slovtsov, 2002. Modeling of thermal-hydrodynamic-chemical processes: some applications to understanding of active hydrothermal systems. *In proceedings of 27th Workshop on Geothermal Reservoir Engineering, Stanford University.*

Kim, J., F. W. Schwartz, J. Shi, and T. Xu, 2003. Modeling the coupling between flow and transport developed by chemical reactoins and density differences using TOUGHREACT. *In Proceedings of TOUGH Symposium 2003*, Lawrence Berkeley National Laboratory, Berkeley, California, May 12–14.

Narasimhan, T. N., and P. A. Witherspoon, 1976. An integrated finite difference method for analyzing fluid flow in porous media, *Water Resources Research*, v.12, p.57–64.

Ontoy, Y., P.l. Molling, T. Xu, N. Spycher, M. Parini, and K. Pruess, 2003. Scaling of hot brine injection wells: supplementing field studies with reactive transport modeling. *In Proceedings of TOUGH Symposium 2003*, Lawrence Berkeley National Laboratory, Berkeley, California, May 12–14.

Pham, M., C. Klein, S. Sanyal, T. Xu, and K. Pruess, 2001. Reducing cost and environmental impact of geothermal power through modeling of chemical processes in the reservoir. *In proceedings of 26th Workshop on Geothermal Reservoir Engineering, Stanford University*, California.

Pruess, K., C. Oldenburg, and G. Moridis, 1999. *TOUGH2 user's guide*, Version 2.0. Lawrence Berkeley Laboratory Report LBL-43134, Berkeley, California.

Robinson, R.A., and R. H. Stokes, 1965. Electrolyte Solutions, the Measurement and Interpretation of Conductance. *Chemical Potential and Diffusion in Solutions of Simple Electrolytes*, 2nd Edition, London, England: Butterworths & Company.

Spycher, N.F., E.L. Sonnenthal, and J.A. Apps, 2003. Fluid flow and reactive transport around potential nuclear waste emplacement tunnels at Yucca Mountain, Nevada, *Journal of Contaminant Hydrology*, v.62-63, p.653-673.

Todaka, N., C. Akasaka, T. Xu, and K. Pruess, 2003. Modeling of geochemical interactions between acidic and neutral fluids in the Onikobe geothermal reservoir. *In Proceedings of 28th Workshop on Geothermal Reservoir Engineering Stanford University*, California, January 27-29.

Todaka, N, and S. Tezuka, S., 2002. Utilization of geochemistry for maintenance of geothermal power plant. Water-dominated reservoir: Onikobe geothermal power plant (Geochemistry for geothermal development)", *Chinetsu*, v.39, p.60-71 (in Japanese).

Verma, A., and K. Pruess, 1988. Thermohydrological conditions and silica redistribution near high-level nuclear wastes emplaced in saturated geological formations. *Journal of Geophysical Research*, v.93, p.1159-1173.

Xu, T., and K. Pruess, 1998. Coupled modeling of non-isothermal multiphase flow, solute transport and reactive chemistry in porous and fractured media: 1. Model development and validation. *Lawrence Berkeley National Laboratory Report LBNL-42050*, Berkeley, California, 38 pp.

Xu, T., K. Pruess, and G. Brimhall, 1999. An improved equilibrium-kinetics speciation algorithm for redox reactions in variably saturated flow systems. *Computers & Geosciences*, v.25(6), p.655 -666.

Xu, T., and K. Pruess, 2001a. On fluid flow and mineral alteration in fractured caprock of magmatic hydrothermal systems. *Journal of Geophysical Research*, v. 106 (B2), p. 2121-2138.

Xu, T., and K. Pruess, 2001b. Modeling multiphase non-isothermal fluid flow and reactive geochemical transport in variably saturated fractured rocks: 1. Methodology. *American Journal of Science*, v. 301, p. 16-33.

Xu, T., E. Sonnenthal, N. Spycher, K. Pruess, G. Brimhall, and J. Apps, 2001. Modeling multiphase non-isothermal fluid flow and reactive geochemical transport in variably saturated fractured rocks: 2. Applications to supergene copper enrichment and hydrothermal flows. *American Journal of Science*, v. 301, p. 34-59.

Xu, T., and Pruess, K., 2001. On fluid flow and mineral alteration in fractured caprock of magmatic hydrothermal systems. *Journal of Geophysical Research*, v. 106 (B2), p. 2121-2138.

Xu, T., E.L. Sonnenthal, N. Spycher, K. Pruess, 2003a. User's guide of TOUGHREACT: A simulation program for non-isothermal multiphase reactive geochemical transport in variably saturated geologic media. *Lawrence Berkeley National Laboratory Report*, Berkeley, California, 200 pp.

Xu, T, J. A. Apps, and K. Pruess, 2003b. Reactive geochemical transport simulation to study mineral trapping for CO_2 disposal in deep arenaceous formations. *Journal of Geophysical Research*, v. 108, No. B2.

Xu, T., E. Sonnenthal, and G. Bodvarsson, 2003c. A reaction-transport model for calcite precipitation and evaluation of infiltration fluxes in unsaturated fractured rock. *Journal of Contaminant Hydrology*, v. 64(1-2) p. 113 - 127.

Wolery, T. J., 1992. EQ3/6: Software package for geochemical modeling of aqueous systems: Package overview and installation guide (version 8.0). *Lawrence Livermore National Laboratory Report UCRL-MA-110662 PT I*, Livermore, California.